

Mechanisms of Fluid-Mud Interactions Under Waves

Robert A. Dalrymple, John H. Trowbridge, Dick K.P. Yue, Samuel J. Bentley, Gail C. Kineke,
Yuming Liu, Chiang C. Mei, Lian Shen, Peter A. Traykovski,
c/o Dept of Civil Engineering
The Johns Hopkins University
3400 North Charles Street
Baltimore, MD 21218
phone: (410) 516-7923 fax: (410) 516-7473 email: rad@jhu.edu

Award Number: N00014-06-1-0718
<http://www.ce.jhu.edu/dalrymple/MURI>

LONG-TERM GOALS

The goals of this project are to investigate the mechanisms for wave dissipation in the presence of bottom mud. These mechanisms are being examined via field measurements in the Gulf of Mexico, laboratory experiments of waves over a mud bottom, and numerical and theoretical analyses. Implementation of these various damping mechanisms into numerical models provides the ability to not only predict wave behavior over mud, but also to infer from the sea surface the nature of the bottom material.

OBJECTIVES

We are measuring wave damping due to mud off the coast of Louisiana, quantifying the dynamics of the bottom mechanisms responsible for the dissipation of wave energy. We are examining different mechanisms for the damping of wave energy by bottom mud in the laboratory and through the use of theoretical and numerical models. These damping mechanisms include the direct forcing of the mud by the wave-induced bottom pressure and velocities; indirect forcing through nonlinear surface wave effects (including wave groups); resonant forcing of interfacial waves at the water/mud interface; damping and shear instabilities in the lutocline; and large scale broadband mechanisms that involve a complex sea state and a combination of the above mechanisms.

APPROACH

The approach involves a field effort, involving experiments within a mud patch offshore the coast of Louisiana; a laboratory effort, examining the above mechanisms in a controlled environment; and a theoretical and numerical approach, with the ultimate objective of providing numerical models that include wave damping over mud.

The field work consists of three field campaigns (a 2007 pilot study and field experiments in the spring of 2008 and 2010) of wave and bottom measurements. The experiments involve the use of bottom-mounted quadrapods that support acoustical instruments to measure the horizontal and vertical

Report Documentation Page				Form Approved OMB No. 0704-0188	
Public reporting burden for the collection of information is estimated to average 1 hour per response, including the time for reviewing instructions, searching existing data sources, gathering and maintaining the data needed, and completing and reviewing the collection of information. Send comments regarding this burden estimate or any other aspect of this collection of information, including suggestions for reducing this burden, to Washington Headquarters Services, Directorate for Information Operations and Reports, 1215 Jefferson Davis Highway, Suite 1204, Arlington VA 22202-4302. Respondents should be aware that notwithstanding any other provision of law, no person shall be subject to a penalty for failing to comply with a collection of information if it does not display a currently valid OMB control number.					
1. REPORT DATE 2011		2. REPORT TYPE N/A		3. DATES COVERED -	
4. TITLE AND SUBTITLE Mechanisms of Fluid-Mud Interactions Under Waves				5a. CONTRACT NUMBER	
				5b. GRANT NUMBER	
				5c. PROGRAM ELEMENT NUMBER	
6. AUTHOR(S)				5d. PROJECT NUMBER	
				5e. TASK NUMBER	
				5f. WORK UNIT NUMBER	
7. PERFORMING ORGANIZATION NAME(S) AND ADDRESS(ES) Dept of Civil Engineering The Johns Hopkins University 3400 North Charles Street Baltimore, MD 21218				8. PERFORMING ORGANIZATION REPORT NUMBER	
9. SPONSORING/MONITORING AGENCY NAME(S) AND ADDRESS(ES)				10. SPONSOR/MONITOR'S ACRONYM(S)	
				11. SPONSOR/MONITOR'S REPORT NUMBER(S)	
12. DISTRIBUTION/AVAILABILITY STATEMENT Approved for public release, distribution unlimited					
13. SUPPLEMENTARY NOTES FY10 Annual Reports of S & T efforts sponsored by the Ocean Battlespace Sensing S & T Department of the Office of Naval Research., The original document contains color images.					
14. ABSTRACT					
15. SUBJECT TERMS					
16. SECURITY CLASSIFICATION OF:			17. LIMITATION OF ABSTRACT SAR	18. NUMBER OF PAGES 18	19a. NAME OF RESPONSIBLE PERSON
a. REPORT unclassified	b. ABSTRACT unclassified	c. THIS PAGE unclassified			

structure of the velocity and concentration and motion of the sediment at the bottom. In addition, a surface buoy provides atmospheric measurements. Two of the quadrapods are located at the seaward and landward ends of the experimental area to provide estimates of the directional wave spectrum and energy flux into and out of the study area. In addition, cores of the seabed have been taken to determine recent depositional history, porosity, and mixing depth. Finally echo-sounding of the entire extent of the measurement profiles was conducted.

Laboratory experiments of waves over muds are being made in two experimental facilities. The first is a shaker table that supports a water/mud tank. This small-scale tank is oscillated to excite wave motion and then stopped so that the decay of the wave motion can be measured for a given mud layer. The second is an 18m long wave tank outfitted with a 10 m long, 10 cm deep mud patch within a false bottom. A string of acoustic and wire wave gages measure the decay of the waves down the tank.

The theory and numerical modeling effort consists of synergistic theoretical consideration, CFD analyses, and direct wavefield simulations (DWS). Regular and multiple scales perturbation analyses with the incorporation of realistic frequency dependent mud rheology have been developed to understand the basic characteristics and damping mechanisms for nearshore wave propagation for relatively simplified wave/mud conditions. CFD analyses based on fully nonlinear Navier-Stokes equation incorporating different mud rheology models are used to investigate the effects of shear instability and turbulence in water and mud layer and to develop equivalent bottom friction coefficient for wave prediction. DWS are developed, based on the integration of the theoretical studies, CFD developments, tank measurements, and field experiments conducted in this project, for the prediction of wavefield evolution over a muddy bottom and topography.

WORK COMPLETED

Three field experiments have been completed and data are being analyzed. Both shipboard measurements (bottom samples, soundings, and multi-beam sonar) and instrumented bottom array experiments have been carried out. In the laboratory, two experimental series are underway in both the wave tank and a shaker table apparatus. The wave tanks tests have shown the development of an instability of the mud/water interface. This instability only appears at certain mud densities in the tank. Wave damping over the mud has been examined for both an incident wave train as well as wave groups. The theory and modeling effort focused on the study and comparison of the effects of different mud rheology on the wave attenuation and on the assessment of the effects of different interaction mechanisms in different conditions by utilizing theoretical methods, CFD analyses, and advanced direct wave simulation (DWS). Specifically, we incorporated existing mud models for perturbation analyses and direct simulations. We performed analytical studies of attenuation of nonlinear long and short waves over Newtonian viscous mud and visco-elastic mud. We conducted CFD analyses of high amplitude waves over thin visco-elastic mud. We developed and integrated modeling of broadband wave attenuation into DWS, compared DWS results with field measurements, and investigated the effect of nonlinear two-layer resonances (water-mud layers) in wave attenuation.

RESULTS

Shipboard measurements--The shipboard measurements were carried out by MURI investigators from Boston College (BC) and Memorial University (MU). The objectives are to provide information on spatial and temporal variability of seabed characteristics (grain size, porosity, mixing depth and

bedding) and to provide snapshots of cross-shelf suspended sediment and stratification in the water column. Similar to 2007-2008 operations, seabed sampling, and water column surveys were conducted prior to the 2010 tripod deployment and upon recovery in mid-March and mid-April, respectively. Two transect lines normal to shore (including the tripod line) were repeated each cruise. A total of ten to twelve multicore sites and ten to twenty hydrographic stations were sampled during each of the two cruises. Acoustic surveys using CHIRP and dual-frequency echo sounder were carried out along the two transect lines with additional alongshore tie-lines

Similar to 2007-2008, 2010 observations document the occurrence of recently deposited, high-porosity sediments that are highly mobile over monthly timescales. Changes in spatial patterns for inventories of the radioisotope Be-7 were observed between cruises, indicating local net sediment deposition and erosion rates equivalent to 0.1-60 kg dry sediment per square meter per month.

Analysis of X-radiographs from this field program has contributed to development of new theory relating hydrodynamics of fluid muds to fabric of sedimentary event beds within fluid-mud deposits (Macquaker, Bentley, and Bohacs, 2010). In situ dynamical observations summarized below and in prior studies suggest that the sedimentary bedding associated with these deposits (rippled sand/silt [a, Fig. 1] overlain by interlaminated silt/clay [b, Fig. 1], which is then overlain by homogeneous clay bed [c, Fig. 1]) is produced by initially turbulent flow in the benthic boundary layer (from waves and currents, unit a) which becomes laminar to transitional as increasing sediment concentrations dampen turbulence. Shear near the base of the mobile fluid mud layer mixes coarser underlying rippled sediment with overlying finer sediment, producing laminations characteristic of these event beds (unit b). Overlying finer suspended sediment, which may be fluid mud, then stabilizes and deposits as flow energy wanes below critical thresholds of motion (unit c).

A custom-built sediment/pore water conductivity probe was constructed at WHOI for deployment on the middle tripod for the 2010 deployment to provide an in situ characterization of sediment porosity throughout the deployment. The probe is mounted above the bed in a frame that was driven by a motor causing the probe to penetrate approximately 0.5 m into a soft seabed every 60 minutes. Two multi-cores collected during the survey at inner shelf locations were sampled by the probe mounted on a tripod while still at the dock prior to deployment. Replicate cores were subsampled and analyzed for bulk density and pore water conductivity (Fig. 2a, b). Although the conductivity probe was damaged early in the deployment, initial results are promising (Fig. 3).

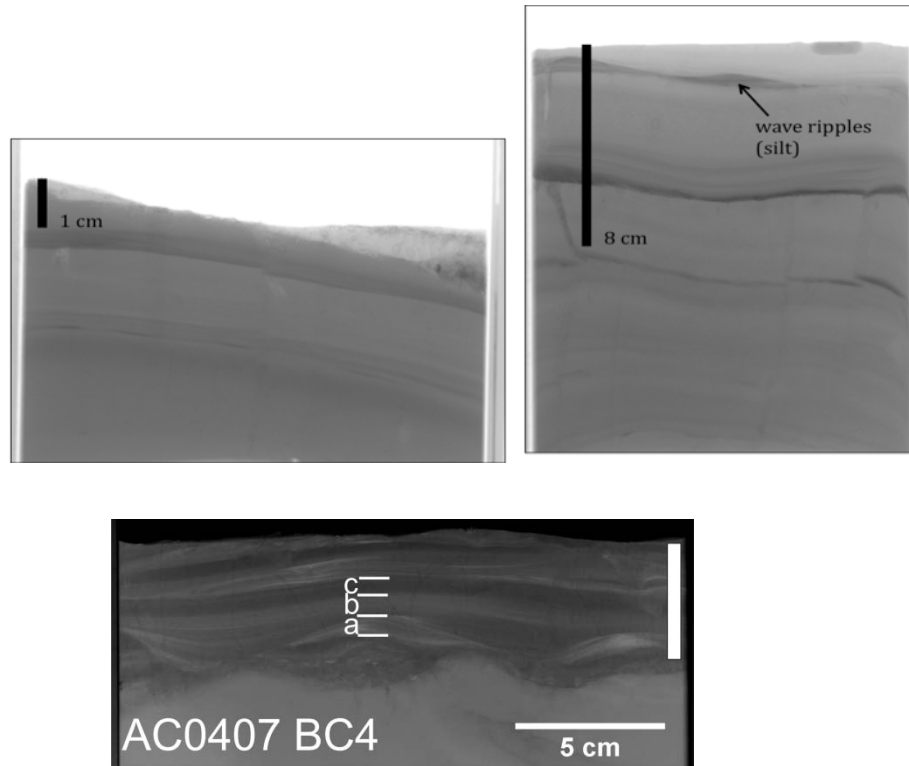


Figure 1. X-radiograph of core AC0407-BC4, showing characteristic bedding. Formation of layers a, b, and c is controlled by boundary layer flow evolution from turbulent to laminar to quiescent (Macquaker, Bentley, and Bohacs, 2010). Multiple similar beds are stacked to produce the observed stratigraphy. Water depth for BC4 is 7m, located along shore-normal transect near of tripod locations. Vertical bar indicates thickness of recently resuspended sediment estimated from 7Be and X-radiographic observation

Conductivity measurements *in situ* and from pore water agree well in the upper fluid part of the core, and gradients in bulk density suggest similar trends with the areas of strong gradients in conductivity. There is somewhat of a mismatch because the measurements were made on different cores from a single multicorer and depths of interfaces between cores may vary due to compaction and settling before sampling. Further laboratory experiments currently underway should provide calibrations for different sediment types, making the probe and driving mechanism a useful tool in muddy environments to provide *in situ* information on fundamental characteristics of the seabed (bulk density or porosity) vertically and over time. These measurements potentially can provide information on concentrations of high concentration bottom layers (currently difficult to do with acoustic and optical sensors) as well as for resuspension depths and compaction rates.



Figure 2. a) Peter Traykovski placing a core beneath the conductivity probe, mounted on a tripod prior to deployment, for a test. b) Boston College students Christie Hegermiller and Mike Cuttler subsampling a replicate core for bulk density measurements to calibrate the conductivity probe

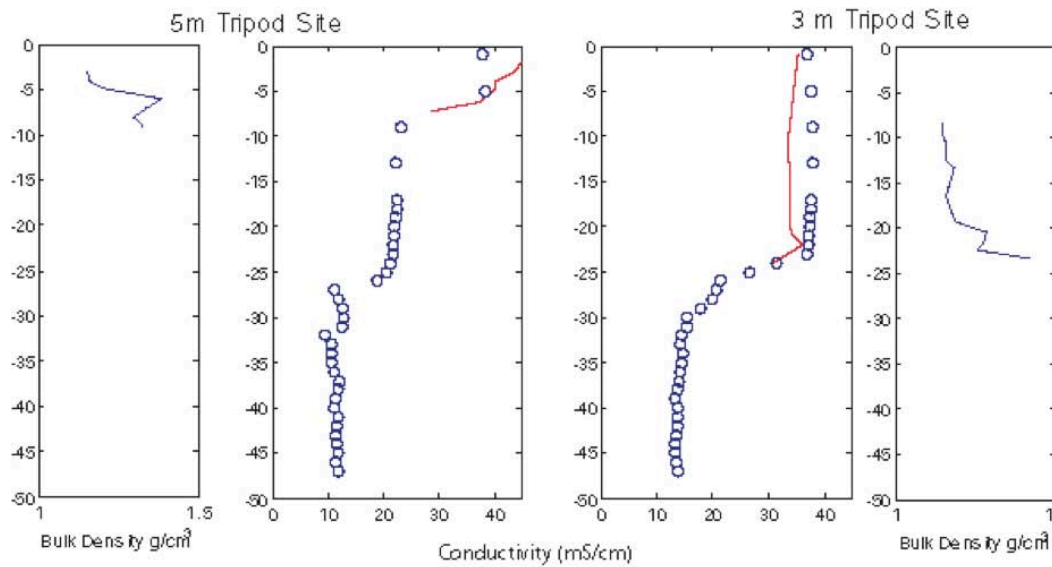


Figure 3. Conductivity probe test. Conductivity measurements from the probe (o) are overlain by conductivity measurements from pore water of a subsampled replicate core in red (b,c). Bulk density measurements from subsampled replicate cores (a,d).

In-situ measurements of seafloor characteristics and wave energy loss--Efforts in 2010 focused both on analysis of data collected in the 2008 field program and on a deployment of instruments in March and April of 2010. The array was located approximately 30 km west of Trinity Shoals and 70 km west of Marsh Island, 5 km east of our 2008 array and in 3 to 7 m water depths, shallower than the 5 to 9 m depth of the 2008 deployment (Figure 4). The new site was located further east to maximize the likelihood of encountering high concentration near bed layers and further inshore to investigate increased dissipation rates in shallow water found by Elgar and Raubenheimer (2008). The outer (7 m water depth) and inner (3 m water depth) tripods contained an upward looking Nortek AWAC (acoustic wave and current) profiler to measure waves, an ABS to measure profiles of suspended sediment and fluid mud concentration, an ADV to measure near bed velocities, and an OBS5 sensor to measure sediment concentration. All sites also contained WHOI built multi-frequency pulse coherent Dopplers. The central site contained a conductivity profiler, which programmed to poke no into the mud every hour and produce estimates of porosity with cm-scale vertical resolution. Unfortunately much of the array was damaged immediately after deployment by shrimp fishing activities. Thus the conductivity probe only took two useful profiles, and the 5 and 7 m depth sites only had usable pressure data for most of the deployment. This pressure data does allow estimates of energy flux and spatial difference in energy flux to calculate divergences and attenuation rates. The 3 m site had 18 days of good data before it was partially damaged with a broken leg (Figure 6 on day 22)

Measurements of attenuation ($\kappa = F_x/F$, where $F = E C_g$ is energy flux) and flux divergence (F_x) from the 2010 data (Figure 5) show a similar pattern to the 2008 data (Figure 6) with maximum attenuation after storms, and maximum flux divergence associated with peak of flux during the storms. Both the attenuation rates and the flux divergence have higher values than in the 2008 data. The maximum attenuation rate is $8e-3 \text{ m}^{-1}$, a factor of two higher than the maximum of $4e-3 \text{ m}^{-1}$ measured in 2008, in deeper water. The flux divergence was also larger in 2010, with a maximum of 1.6 W/m with 1.5 m offshore wave heights, compared to 1.2 W/m with 2.0 m offshore wave heights in 2008. This is qualitatively consistent with observations of Elgar and Raubenheimer (2008) who measured attenuation rates increasing shoreward with a depth raised to the -3.4 power dependence. Further analysis of the 2010 is underway.

In the recent analysis of the 2008 data we have focused on quantifying dissipation mechanisms when the flow appears to be turbulent during the peak of the storm. Data from a 20° off vertical Doppler beam combined with an adjacent vertical beam was also used to measure the vertical structure of horizontal velocity. At 1 mHz this system was able to make velocity profiles through the water and into the mud layer, producing unique insights into the mechanisms of dissipation. The velocity profile data (Figure 7) shows that during periods of maximum wave attenuation, the wave boundary layer expands to fill the entire mud layer, consistent with theory that suggests attenuation should be maximized when the velocity boundary layer thickness ($\delta = \sqrt{2\nu/\omega}$) is approximately equal to the mud layer thickness (h_m), i.e. $h_m/\delta = 1.4$. The data also shows that turbulence in the mud layer, as measured by the high frequency fluctuations in vertical velocity, is highly damped compared to the overlying water during the period of maximum spatial attenuation rate (Figure 8). This indicates that two layer models with a high viscosity lower layer are probably appropriate for this situation. In contrast, during the period of maximum total dissipation turbulence in the wave boundary layer is much higher than in the overlying water. During this period a two layer model is not appropriate and a model that parameterizes (or resolves) turbulence is required. Models based on two-layer theory (e.g.

Dalrymple and Liu, 1978) can fit the measured velocity data with a viscosity of $0.01 \text{ m}^2/\text{s}$, four orders of magnitude greater than clear water. Viscosity an order magnitude less than 0.01 predicts a boundary layer that is much thinner than the measured velocity structure and mud layer thickness, and viscosity an order magnitude greater than 0.01 predicts a boundary layer that is much thicker than the measured velocity structure with too much shear at the mud water interface.

During the period from peak of the storm to about halfway through the waning stages the velocity profiles in the mud can be fit with a profile consistent with a viscosity of $0.001 \text{ m}^2/\text{s}$. The turbulent spectra of vertical velocity during this period show a $f^{-5/3}$ dependence at frequencies above the swell band in the water consistent with turbulent flow (Figure 9&c). However, estimates of turbulent dissipation calculated using the inertial dissipation method with the vertical velocity spectral predict a dissipation rate that is a factor of 20 lower than the observed flux divergence. Further investigation into the spectra using conditional averaging, whereby spectra containing less than 20% of the total energy in the $f > 0.4 \text{ Hz}$ band are averaged together, show spectra that are consistent with laminar flow as in Figure 5. Thus, it appears the flow is transitioning from laminar flow in between wave groups to turbulent flow during groups and that the much more dissipative laminar dissipation mechanism is responsible for the flux divergence that is much higher than can be accounted for by turbulent dissipation.

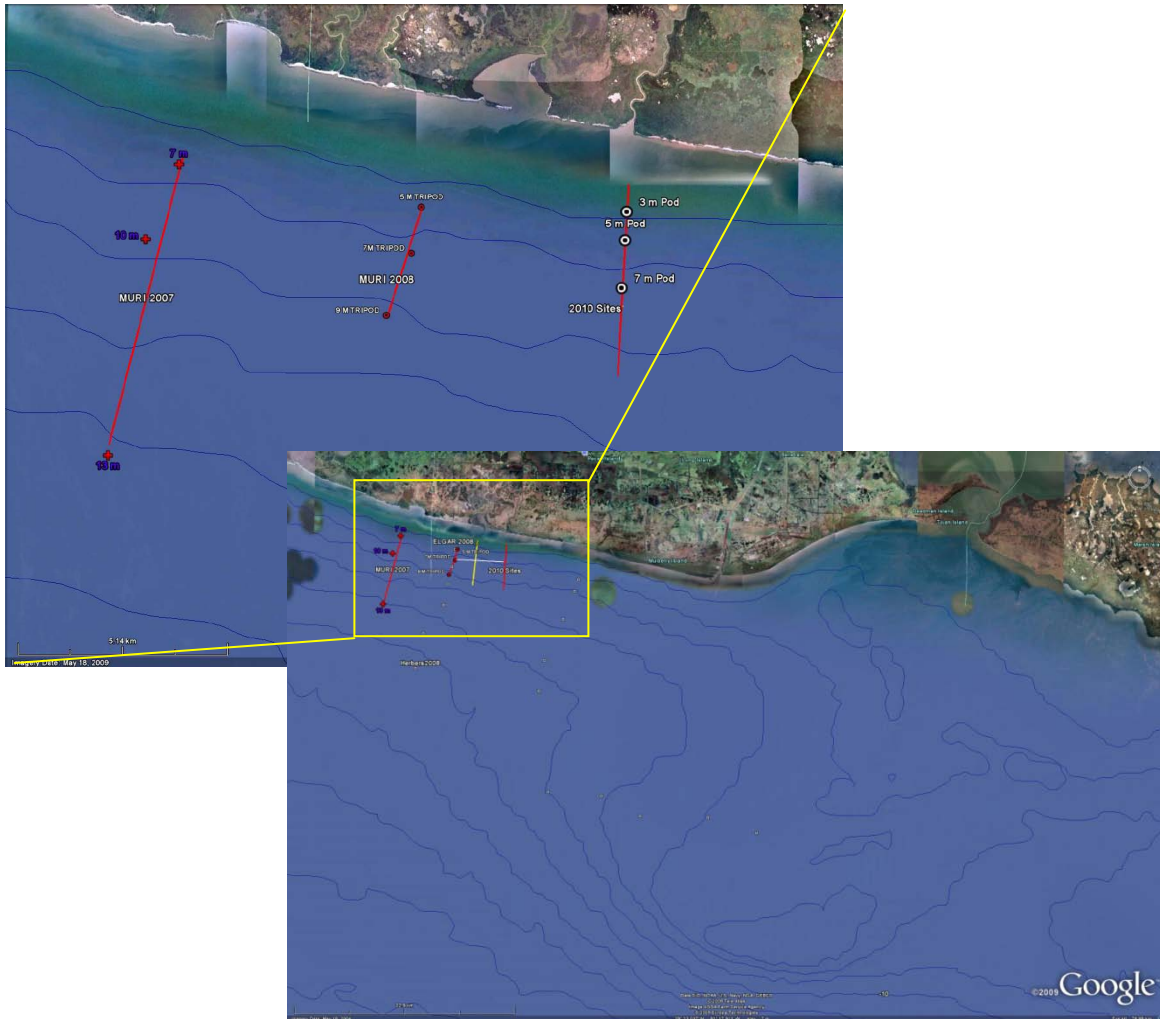


Figure 4. Deployment locations in 2007, 2008 and 2010. In 2010 we moved further east to increase the likelihood of encountering high concentration near bed layers, and further inshore to investigate increase dissipation rates in shallow water.

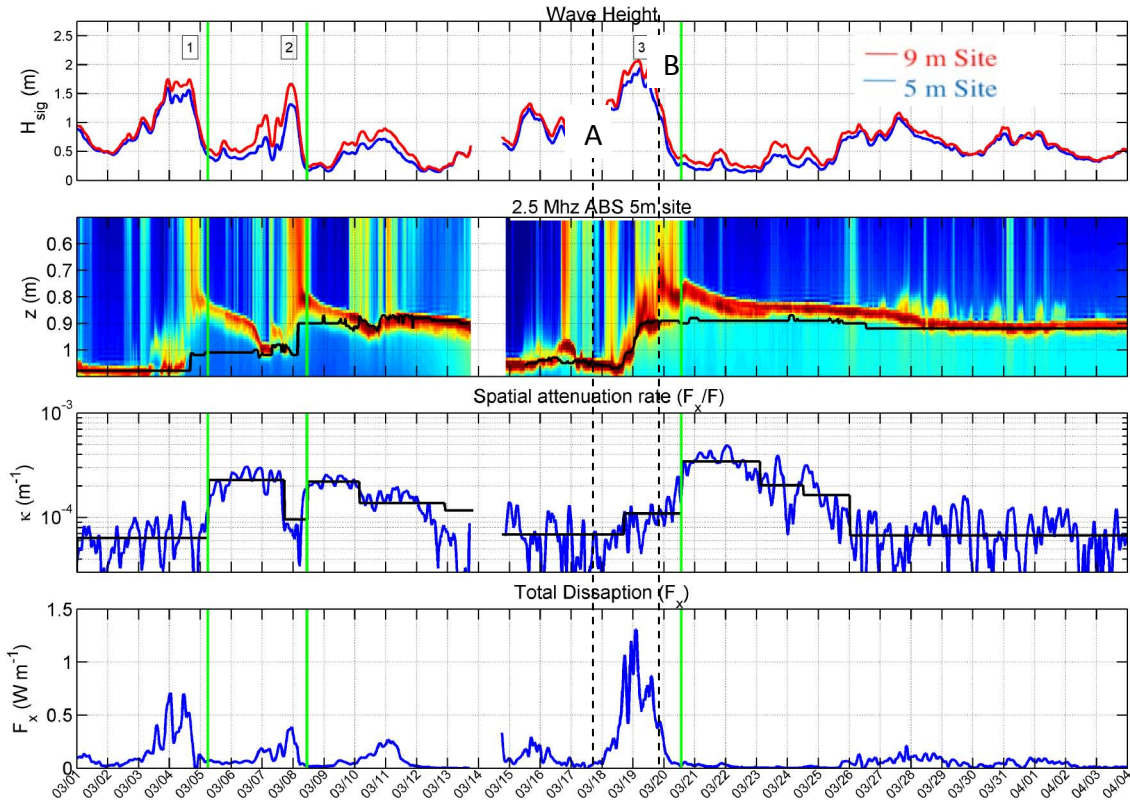


Figure 5. Data from the 2008 Deployment: a) Time series of $H_{1/3}$ from the 5 m (blue) and 9 m (red) isobath sites. The three wave events with $H_{1/3} > 1.5$ m are labeled 1, 2 and 3. b) Burst averaged 2.5 MHz ABS data with the consolidated mud bottom, calculated from the 1 MHz ABS data shown as a black line. The color is proportional to backscattered intensity, corrected to account for sediment attenuation in the water column. c) Attenuation F_x/F calculated from the 9 m and 5 m site (blue) and a stepwise low pass fit (black) and d Flux convergence F_x calculated from the 9 m and 5 m site.

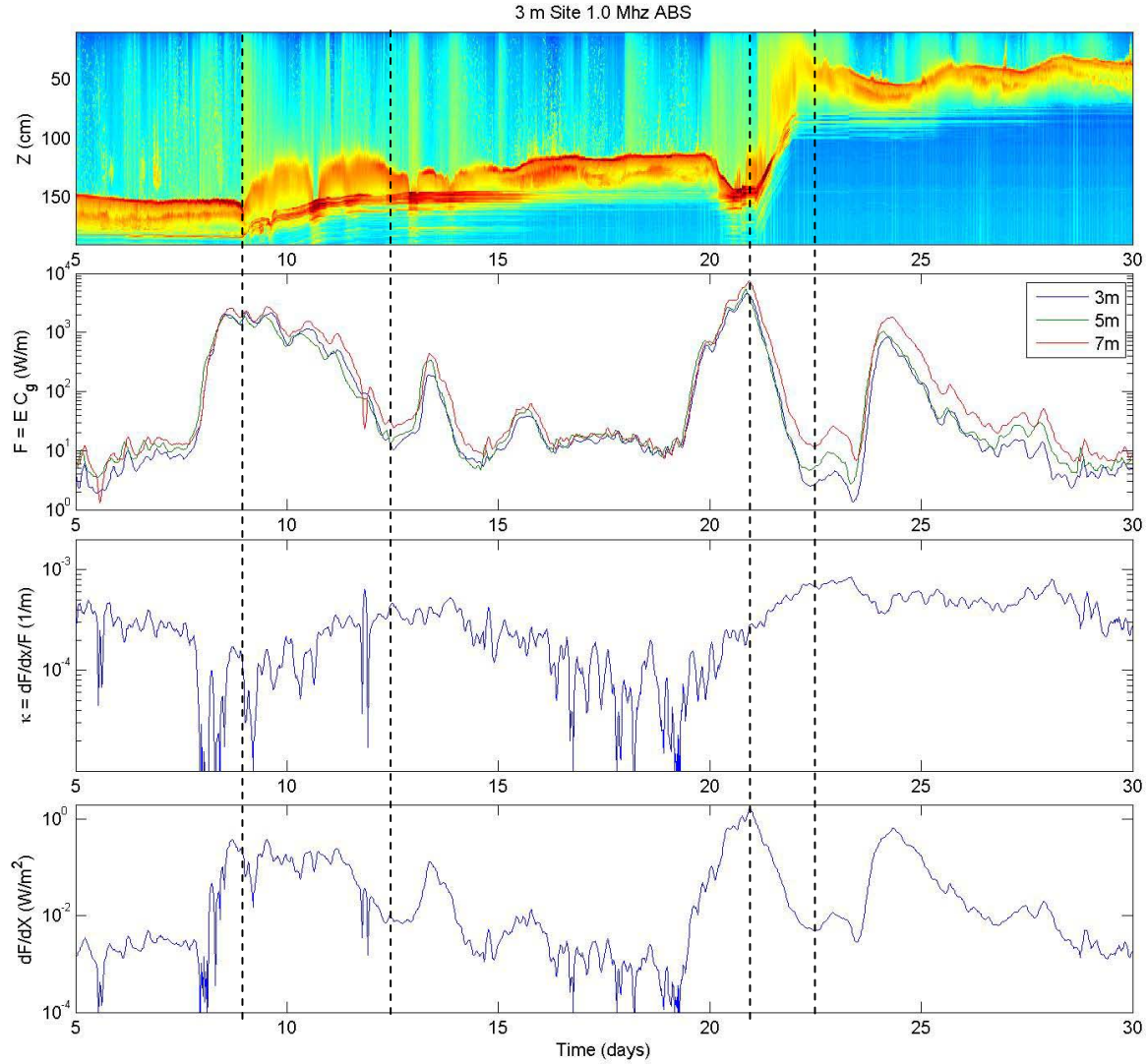


Figure 6. Data from the 2010 deployment a) Burst averaged 1.0 MHz ABS data from the 3m site with multiple acoustic reflectors in the mud layers visible. The color is proportional to backscattered intensity, corrected to account for sediment attenuation in the water column. b) Time series of energy flux ($F = E C_g$) from the 3 m (blue) and 5 m (green) and 7 m (red) isobath sites c) Attenuation $\kappa = F_x/F$ calculated from the 7 m and 3 m site (blue) and d) Flux convergence F_x calculated from the 7 m and 3 m site. The timing of the increased κ after wave events is similar to 2008 data, but attenuation levels are higher in this shallow water deployment both during and after the wave events

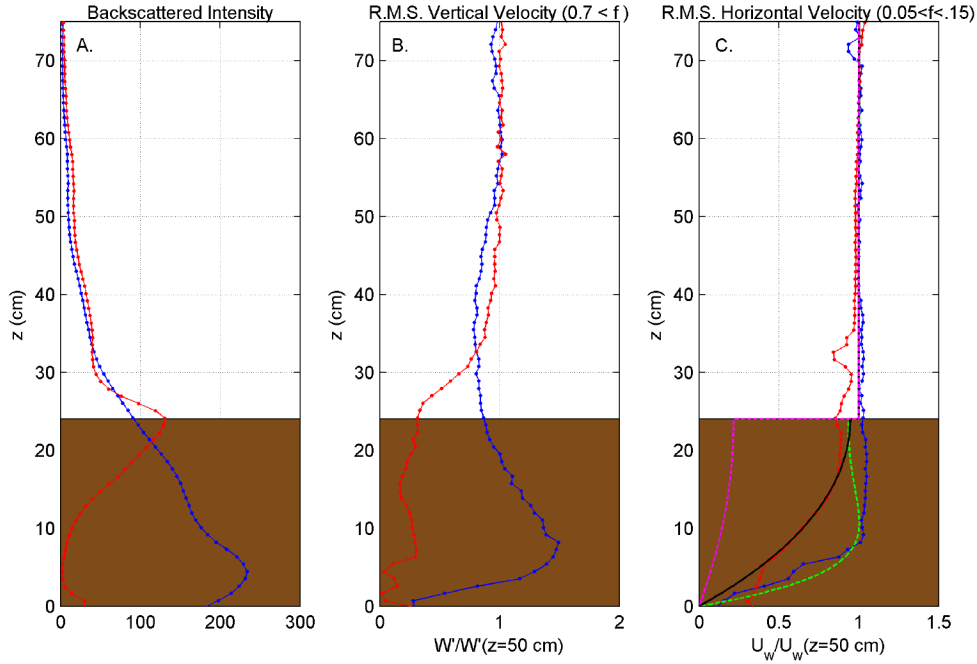


Figure 7. Vertical Profiles of A. backscattered intensity, B. high frequency R.M.S. vertical velocity normalized by free stream velocity, and C. wave band horizontal velocity. The red lines are from the period of maximum spatial attenuation rate (F_x/F , vertical line labeled B in figure 1), and the blue lines are from the period of maximum wave energy and maximum total dissipation (F_x , vertical line labeled B in figure 1). Two layer model results for viscosities of 0.1 (magenta), 0.01 (black) and 0.001 (green) are superimposed on the horizontal velocity plot (C.) indicating the velocity during the period of maximum attenuation is best fit with a viscosity of 0.01 m²/s.

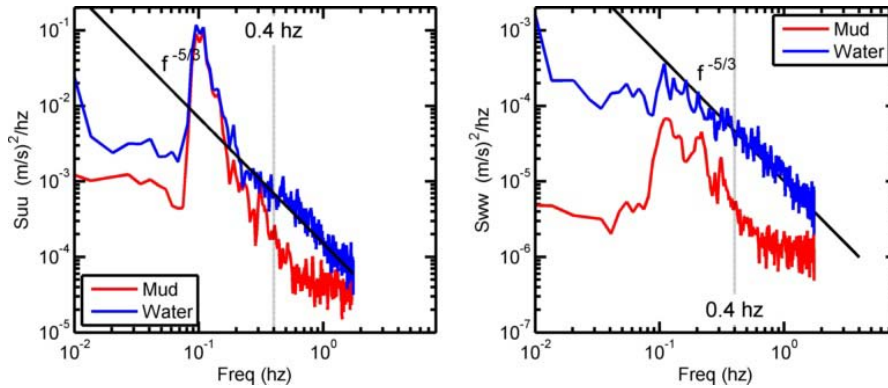


Figure 8. a) Horizontal velocity spectra in the overlying water (blue) and mud (red) showing the swell band variance (0.7 Hz to 0.2 Hz) is approximately equal in both the mud and water. b) Vertical velocity spectra show a $f^{5/3}$ dependence at frequencies above the swell band in the water consistent with turbulent flow; however, in the mud layer there is a rapid fall off in spectral energy above 0.4 Hz to levels defined by the instrument noise floor indicating laminar flow in the mud.

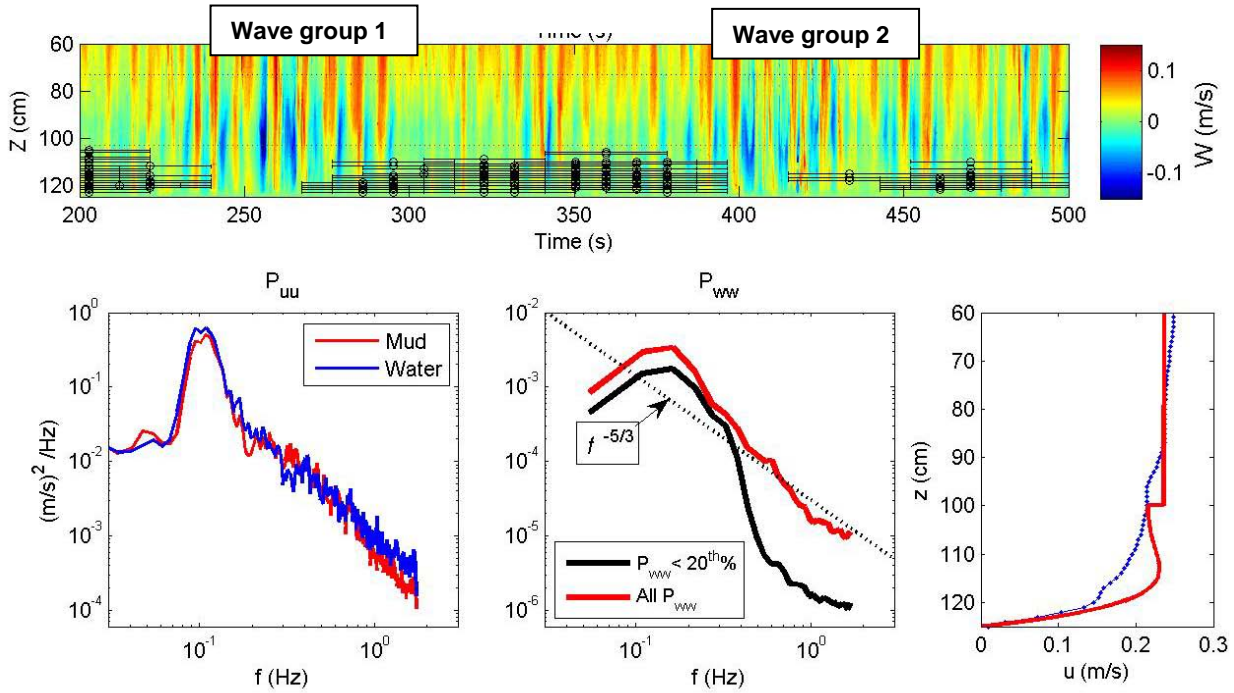


Figure 9. a) Vertical velocity time series with periods of low high frequency variability in the mud layer ($z > 90$ cm) indicated with horizontal lines b) Spectra of vertical velocity in the overlying water and the mud with a $f^{-5/3}$ dependence at frequencies above the swell band in the water consistent with turbulent flow. c) Conditionally averaged spectra with spectra containing less than 20% of the total energy in the $f > 0.4$ Hz band averaged together. These low energy spectra have a rapid fall off in spectral energy above 0.4 Hz to levels defined by the instrument noise floor indicating laminar flow in the mud in between wave groups, and turbulent flow during the wave group

Laboratory Experiments-- We have conducted a series of experiments and analyses into the mechanics of wave damping over mud. The main set of experiments have taken place using the 18 m long wave tank. A 10 m recessed section of the tank contains a layer of kaolinite clay. Testing has consisted of three phases. First, a series of monochromatic wave trains were produced over a range of wave frequencies and in a range of water depths to assess the damping behavior with respect to a variety of parameters such as wave frequency, wave height and water depth. Damping was assessed by comparing wave heights at various longitudinal locations in the tank. Second, “wave beats” were created by superimposing waves of two frequencies to create a longer envelope. Third, the wave maker was used to generate a representative random sea condition, based on the Pierson-Moskowitz sea spectrum. For this type of testing, damping is assessed by measuring wave energy flux over a period of time at various longitudinal locations in the tank. Spectral analysis was also performed at these locations to track changing spectral energy, as previous studies have hypothesized mechanisms of energy transfer between waves of different frequencies.

For monochromatic waves, significant wave damping was observed with upwards of 50% amplitude attenuation over the 10 m mud section, or about 6 wavelengths ($kh > \pi$). Deep water cases ($kh > \pi$) were also tested as there has been recent indications that damping can occur in deep water. Moderate wave attenuation was observed for some cases with a kh of greater than 4, though some cases with similar kh values resulted in negligible attenuation. The depth of the mud layer was found to be significant as the wave damping occurs where the mud layer is located, not necessarily where the bottom is located. A second phase of experiments examined wave groups, in which two frequencies, both of which were high enough to produce deep water waves, were superimposed to produce a “beat” frequency that corresponded to a shallow water wave. It was observed that the damping produced with wave beats was essentially the same as the damping observed with the individual wave frequencies and no additional effects were measured as a result of the superposition.

Interfacial waves were observed during some wave conditions. The interfacial waves tend to only form when the lutocline is near the free surface and take on a peculiar form that gives the water surface a corrugated appearance (Figure 12). Through careful analysis of these tests, it has been concluded that the waves are the result of a resonant three-wave interaction in which a monochromatic surface wave incites a pair of nearly-orthogonal propagating interfacial waves.

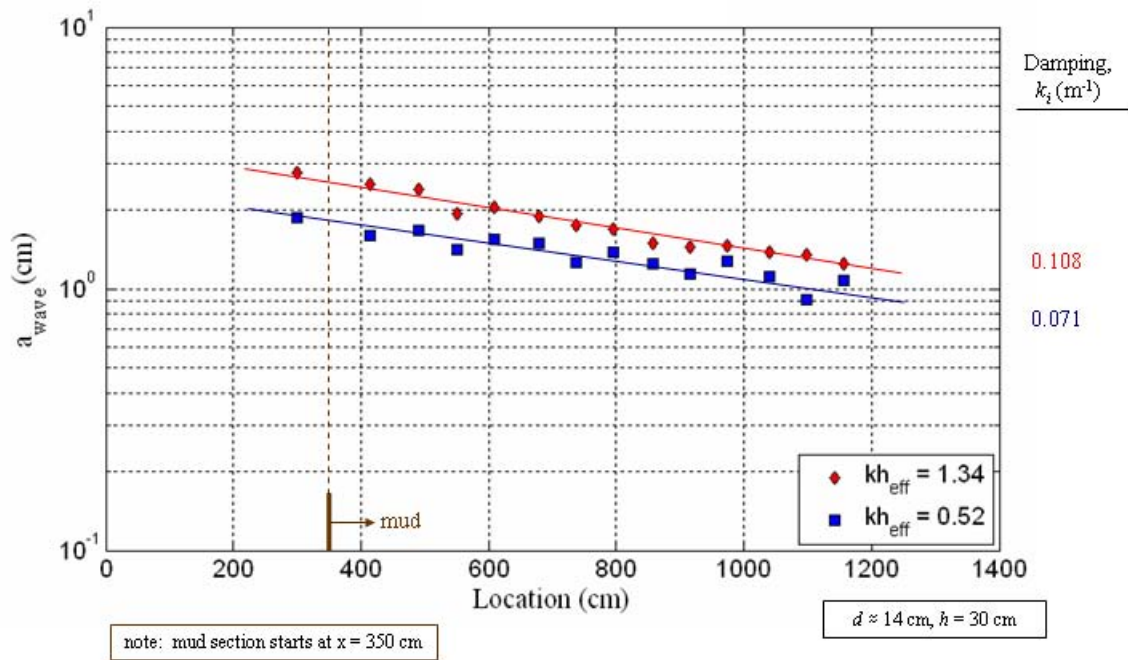


Figure 10. Deep water damping tests using waves with periods of 1 second (red) and 2 seconds (blue). Note: kh_{eff} is the value of kh using the depth to the mud layer for h .

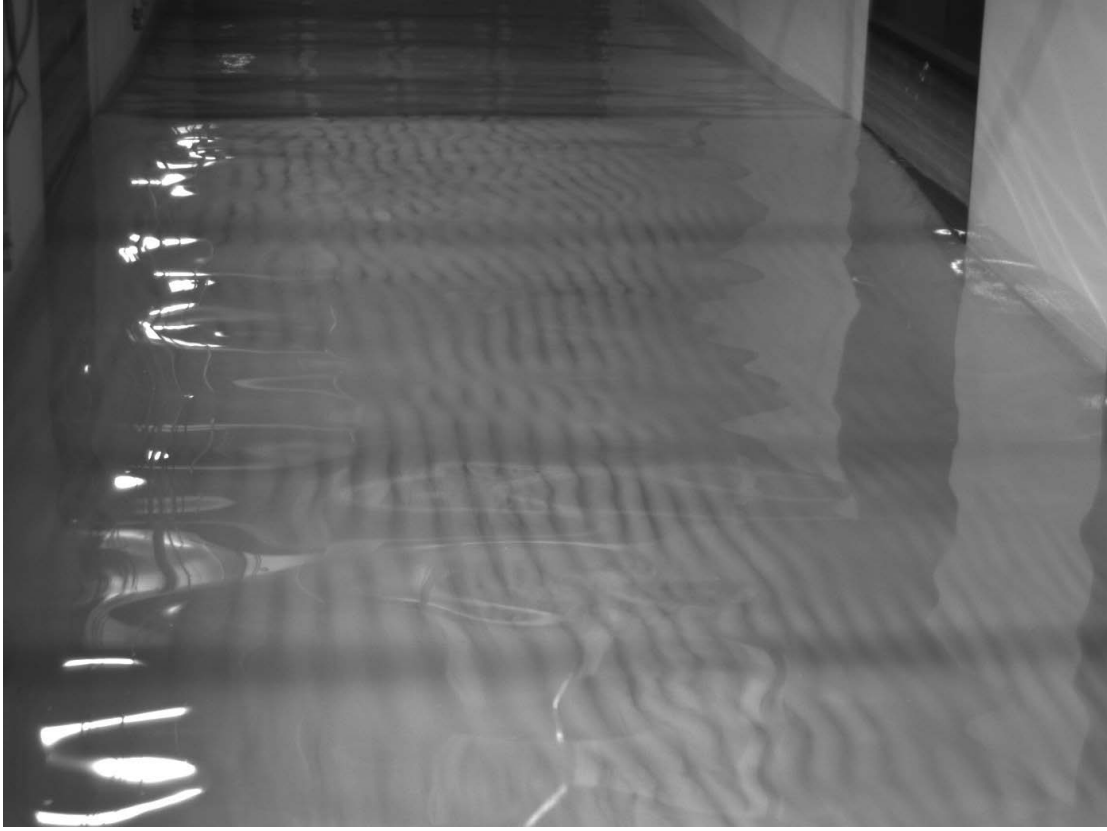


Figure 11. Observation of interfacial waves when the lutocline is near the water surface.

Theoretical and Numerical Modeling--A theoretical study is carried out for predicting the effects of fluid mud on waves in near-shore waters with emphasis on two realistic features of fluid mud in coastal waters: the viscoelastic rheology and the small thickness of the mud layer. The theory is developed based on a multiple-scale perturbation analysis of nonlinear wave-mud interactions. The analysis is performed for moderately shallow mud and very shallow mud. Both horizontal and gently sloping seabeds are considered. In the case of moderately shallow mud, the interface displacement is found to be relatively large though much smaller than the free surface displacement. The length scale of spatial attenuation of the free surface is found to be of the order $O(1/kh)$ times the wave length, where k is the wavenumber and h is the water depth. In particular at the second-order there is a drift velocity (mass transport) in the mud layer so that waves push mud slowly forward. In the second case of very shallow mud, the interface displacement is found to be very small. As a result, dissipation is much weaker and waves are damped out more slowly. If the seabed is horizontal the decay distance is of the order distance $O(1/k^2h^2)$ times the wavelength. Over such a distance harmonic generation due to nonlinearity becomes effective so that the wave spectrum broadens. Over a sloping beach, the wave evolution depends on the slope, or equivalently, the width of the beach. If the slope is small harmonic generation is evident. If the slope is large, waves are damped before energy interchanges between first and higher harmonics take place. Figure 12 shows a sample result of the spatial evolution of wave harmonic amplitudes $A_m(X)$ for $m = 1, 2, 3, \dots$, for visco-elastic mud (in Gulf of Mexico) of constant mean depth over a plane beach of slope s , where $X = 1/s$ is the dimensionless distance with $X = 0$ being the start of the slope and $X = 1/s$ the shoreline. For this result, rheological data is obtained from laboratory experiments by the laboratory team in this project.

A suite of advanced CFD capabilities with the incorporation of various mud rheology models and turbulent effects are developed and applied to simulate the coupled wave and mud motions. The simulations can be performed on moving boundary-fitted grid to have fine resolution of the boundary layers, or on fixed Eulerian grid with two level-set functions to address violent interfacial phenomena. A numerical capability for stratified flows is also developed. Various models for the mud flow are implemented, including viscous fluid model, visco-elastic models such as Voigt and Maxell models, and Bingham plastic model. CFD simulations are validated by comparisons with existing measurements and theoretical results. We apply the CFD simulations together with DWS to investigate the nonlinear wave effects on the damping rate of waves over various muddy bottoms. Figure 13 shows a sample result for the dependence of the damping rate on the wave steepness. For this example, the wave has a frequency of 2 Hz. The depths of water and mud are 3 m and 0.3 m, respectively. The water has a density of 1000 kg/m^3 and a kinematic viscosity of $10^{-5} \text{ m}^2/\text{s}$. The mud has a density of 1300 kg/m^3 and a kinematic viscosity of $0.05 \text{ m}^2/\text{s}$. The wave damping rate is compared among the predictions by the linear theory (MacPherson 1980), CFD computations, and DWS. For small wave steepness ka , the agreement among them is excellent. For large ka , both CFD and DWS results show that nonlinearity increases the wave damping rate. Stronger nonlinear effects are predicted by CFD. This is because the DWS captures surface-mud wave nonlinearities while the CFD further captures viscous effects and the associated nonlinear processes.

We integrate the theoretical and CFD studies of wave attenuation by interaction with mud flow into direct wavefield simulations (DWS) for predicting the evolution of nonlinear broadband wavefield over near-shore muddy seabeds. We obtain comparisons and cross-validations between existing theories, CFD and DWS for wave dissipation by viscous mud and visco-elastic mud. We compare the prediction of broadband wave spectrum evolution by nonlinear DWS with that by the linear theory to characterize the effect of nonlinear wave interactions upon wave damping. In particular, with DWS computations, we quantify the mechanism and dependence for the damping of short waves over muddy bottom through energy transfer to long waves via near resonant wave-wave interactions. We apply DWS to obtain various comparisons in wave spectrum evolution over muddy seabeds between DWS predictions and available field measurements (Wells & Kemp 1986; Elgar & Raubenheimer 2008). The results show that one-layer resonant (non-linear) mechanism plays a significant role in development and dissipation of ocean spectrum in shallow muddy waters, and resonant surface-interface interaction in a two-layer fluid-over-mud model may lead to strong dissipation of surface wave energy. Our results also indicate that proper modeling and calibration of mud properties is of critical importance for a reliable prediction of ocean waves over a muddy seabed as the mud properties vary strongly in time and space. Figure 14 presents sample comparisons of the WDS predictions and the field measurements at Louisiana coast (Elgar & Raubenheimer (2008) and Suriname coast (Wells & Kemp 1986). Mud properties (BOMP1) in DWS are obtained by calibration with field wave measurements at Louisiana at 4/14/08, 3:00 CST. DWS prediction (with BOMP1) compares quite well with the field measurement at the same place about 4 hours later (at 4/14/08, 7:00 CST). The DWS predictions are totally deviated from the field measurements at the same place about 13 hours earlier or at Suriname coast, a different place.

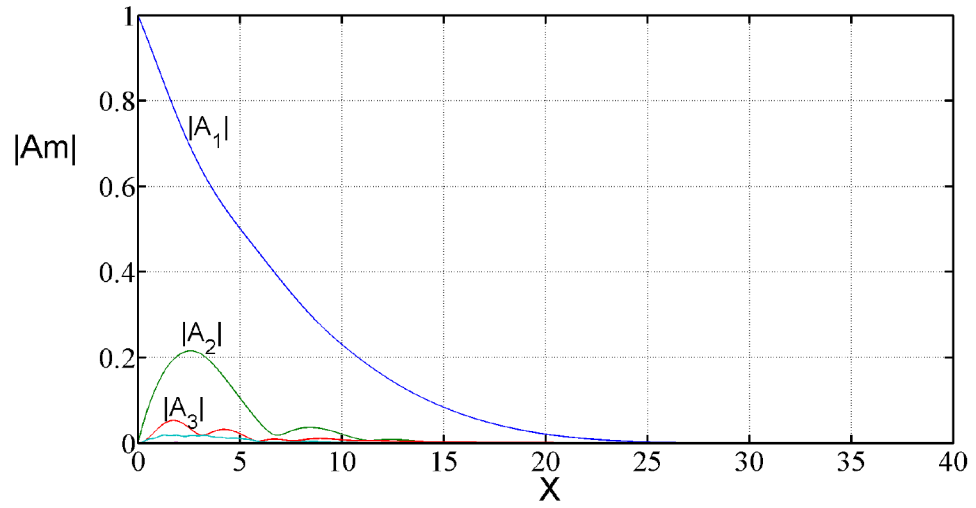


Figure 12. Evolution of harmonic amplitudes on a sloping muddy beach of slope 1/40 for fluid mud from Gulf of Mexico.

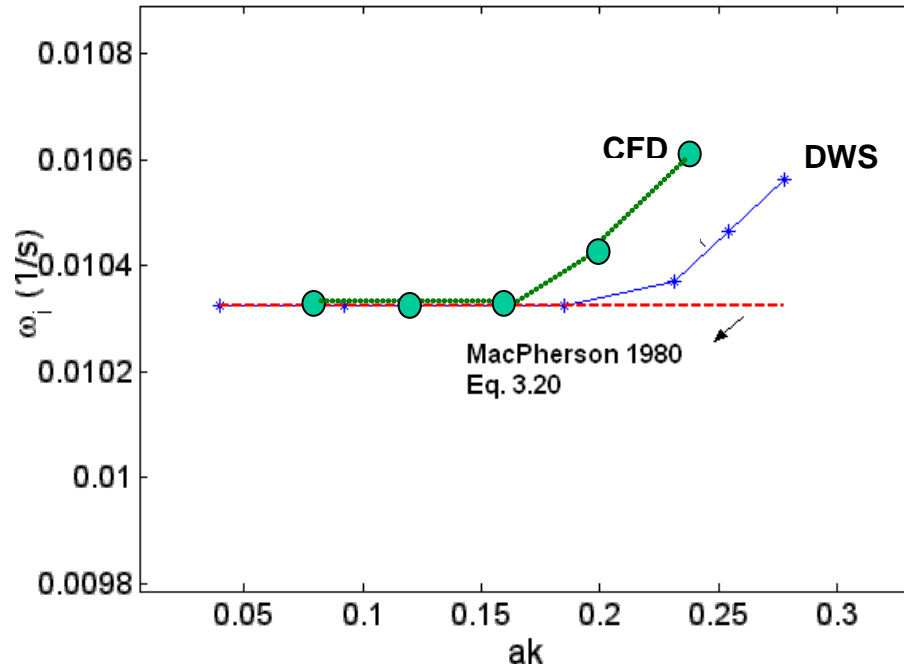


Figure 13. Variation of wave damping rate with wave steepness. Shown are the comparisons among the predictions by the linear theory (MacPherson 1980), CFD, and DWS.

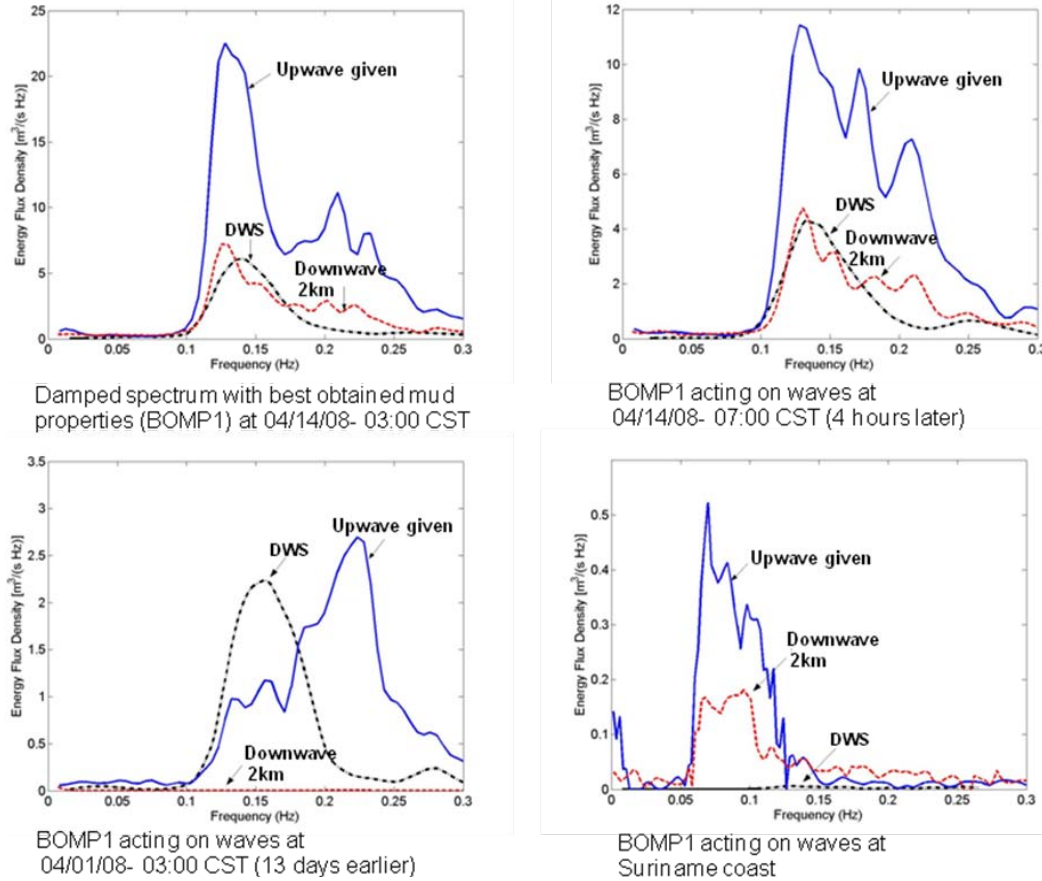


Figure 14. Comparisons of DWS predictions and field measurements of ocean wave evolution over muddy seabed at Louisiana coast (Elgar & Raubenheimer 2008) and Suriname coast (Wells & Kemp 1986). Solid line: measurement of upwave used as given boundary condition in DWS simulation; dash line: measurement at 2 km downwave; dash dot line: DWS prediction of 2km downwave.

IMPACT/APPLICATIONS

The results of this combined field/laboratory/theory/modeling effort are field and lab data for model verification and testing and models for the propagation of water waves over regions of bottom mud. The dissipation due to a variety of mechanisms is included in the models; however, the most likely mechanisms will be determined from the field experiments. Laboratory experiments will provide data to elucidate the mechanisms of energy transfer from the waves to the sediment.

REFERENCES

- Dalrymple, R.A. and Liu, P. L.-F. 1978 Water waves over soft muds: a two-layer fluid model. *J. Phys. Ocean.*, Vol. 8, pp. 1121-1131.
- Elgar, S. and Raubenheimer, B. 2008 Wave dissipation by muddy seafloors, *Geophysical Research Letters*, Vol. 35 (7), 1-5.

- Jiang, F. and Mehta, A. 1995 Mudbanks of the southwest coast of India. IV: Mud visco-elastic properties. *Journal of Coastal Research*, 11 (3), 918–926.
- Macquaker, J., Bentley, S.J., and Bohacs, K., 2010, Wave enhanced sediment-gravity flows and the dispersal of mud across continental shelves: a reappraisal of physical sedimentary processes operating in distal, “low energy” settings and their stratal record. *Geology* 38: 947-950.
- MacPherson, H. 1980, The attenuation of waves over a non-rigid bed, *Journal of Fluid Mechanics*, 97:4, 721-742.
- Mei, C.C., Krotov, M., Huang, Z.H. and Aode, H. 2010 Short and long waves over a muddy seabed. *J. of Fluid Mech.* (643), 33-58.
- Wells, J. T., and Kemp, G. P. 1986, Interaction of surface waves and cohesive sediments: field observations and geologic significance, in Mehta, A. J., ed., *Estuarine Cohesive Sediment Dynamics*: New York, Springer-Verlag, 43-65.

PUBLICATIONS

- Alam, M.R., Liu, Y. and Yue, D.K.P. 2010 Oblique sub- and super-harmonic Bragg resonance of surface waves by bottom ripples. *J. of Fluid Mech.* (643): 437-447
- Mei, C.C., Krotov, M., Huang, Z.H. and Aode, H. 2010 Short and long waves over a muddy seabed. *J. of Fluid Mech.* (643), 33-58.
- Shen, L. 2010 Numerical study of wave-turbulence interaction. *In Notes on Numerical Fluid Mechanics and Multidisciplinary Design: Turbulence and Interactions*, Springer.
- Macquaker, J., Bentley, S.J., and Bohacs, K., 2009 Wave enhanced sediment-gravity flows and the dispersal of mud across continental shelves: a reappraisal of physical sedimentary processes operating in distal, “low energy” settings and their stratal record. *Geology* [submitted]
- Bentley, S.J., Maas, K.A., Brandstatter, S., Johnson, S., and Kineke, G., 2008, Depositional Processes and Sediment Properties of Fluid Muds on the Inner Shelf: Western Mississippi Delta, Louisiana, USA. AGU Chapman Conference on the Physics of Wave Interactions with Fluid Mud, Amelia Island, Florida, November 2008.
- Brandstatter, S., Bentley, J., Johnson, S., Kineke, G., and Lermon, M., 2009, Be-7 inventories as a tracer for sediment movement on the inner shelf: western Atchafalaya River Delta, Louisiana. Spring Meeting Geological Association of Canada Newfoundland and Labrador Section, March 2009.